Hexrotor UAV Platform Enabling Dextrous Aerial Mobile Manipulation

Guangying Jiang[1] and Richard Voyles[2]

[1] University of Denver, Denver, Colorado, USA
gjiang2@du.edu
[2] Purdue University, West Lafayette, Indiana, USA
ricard.voyles@du.edu

Abstract

Mobile manipulation is a hot area of study in robotics as it unites the two classes of robots: locomotors and manipulators. An emerging niche in the field of mobile manipulation is aerial mobile manipulation. Although there has been a fair amount of study of free-flying satellites with graspers, the more recent trend has been to outfit UAVs with graspers to assist various manipulation tasks. While this recent work has yielded impressive results, it is hampered by a lack of appropriate testbeds for aerial mobile manipulation, similar to the state of ground-based mobile manipulation a decade ago. The Collaborative Mechatronics Lab is addressing this instrumentation gap with the development of a dexterous UAV platform to eventually host a low-cost, lightweight Stewart-Gough platform that can be combined as a macro/micro mobile manipulation system. Based on the concept of force closure (a term from the dexterous manipulation community), the new type of dexterous, 6-DoF UAV provides the unique capability of being able to resist any applied wrench, or generalized force-torque. Typical helicopters or quadrotors cannot instantaneously resist or apply an arbitrary force in the plane perpendicular to the rotor axis, which makes them inadequate for complex mobile manipulation tasks. We have developed a hexrotor UAV that can exert arbitrary wrenches in the 6-DoF force/torque space. In this paper, we describe the importance of force closure for mobile manipulation, explain why it is lacking in current UAV platforms, and describe how our hexrotor provides this important capability as well as exhibiting holonomic behavior. We also describe the results of a staged peg-in-hole task that exerts forces without pitching and rolling the UAV, reducing uncertainties.

1 Introduction

The field of mobile manipulation combines two broad classes of robots, locomotors and manipulators, yet the potential impact is greater than the sum of the parts. Aerial mobile manipulation is an emerging field within mobile manipulation for which the locomotor is a UAV (unmanned aerial vehicle) [11, 15, 1, 9]. The popular quadrotor has become the main UAV of choice in robotics research, due to its ease of control and low cost. The added mobility and access that quadrotors provide brings a new dimension to the study of mobile manipulation and new challenges, as well.

One of the greatest challenges that UAVs, in general, introduce, and quadrotors in particular, is the inability to instantaneously exert forces in the plane. Quadrotors are non-holonomic; in order for them to move forward or sideways, they first have to pitch the entire body of the quadrotor to direct the thrust vector in the desired direction. What this means for aerial mobile manipulation is that the quadrotor cannot resist an arbitrary generalized force/torque. In the parlance of the dexterous manipulation community, it lacks "force closure". In fact, in one of the first attempts to use a UAV to interact physically with its environment, Albers et al had to add an auxiliary actuator to maintain contact so Newton' Third Law of equal and opposite reaction would not immediately push the UAV away [2].

To solve this specific problem more elegantly, we are developing a hexrotor UAV that can instantaneously resist arbitrary forces – in other words, it provides force closure. To perform precise and effective mobile manipulation, this is a property that any locomotor must have, be it ground-based, water-based, or air-based. To achieve this, the thrusters of our hexrotor are canted so that the combined thrust vectors span the space of Cartesian forces and torques. This adds little cost or complexity to a conventional hexrotor.

The focus of this paper is on the hexrotor platform and its suitability as a future carrier of a manipulator for aerial mobile manipulation. Although we do describe the preliminary design of a low-cost, lightweight hexmanipulator (6-DoF Stewart-Gough platform) we have in development, that is not the focus of this paper.

1.1 Force and Form Closure

Force closure, as defined by Rimon and Burdick, is the ability of a mechanism to directly resist any arbitrary wrench (combination of force and torque) applied to it. A "force closure grasp" in the dextrous grasping literature [13, 3], is a grasp of an object that can resist an arbitrary wrench applied to the object. This class of grasps is important to the dexterous manipulation community but is often ignored by the mobile manipulation community because of the large mass of the mobile base and other issues have greater priority.

However, aerial mobile manipulation is a newly emerging field and the floating nature of aerial platforms and the highly compliant nature of their positioning brings the issue of force closure to the fore. Force closure for arbitrary rigid objects in 3-space requires six controllable degrees of freedom in force-torque space to truly accomplish. Most piloted helicopters and unmanned aerial vehicles manipulate objects by hanging them from a line and/or employ fewer than six vehicles [12], severely limiting the range of wrenches that can be applied to the object. The quadrotor teams of Mellinger et al [11] rigidly clamp to the manipulated object but, due to their design, they can only apply limited forces and torques. In generalized force space, they are effectively degenerate.

Furthermore, it is not sufficient to simply attach a 6-DoF manipulator to the bottom of a quadrotor or other degenerate aerial platform, as this does not guarantee force closure. While a 6-DoF manipulator can exert arbitrary wrenches when grounded, if the base upon which it is mounted cannot resist an arbitrary wrench, the combination remains degenerate.

1.2 Related Works

People have started to apply helicopters and quadrotors to mobile manipulation. Unstable dynamics of the vehicle and coupled object-aircraft motion while grasping objects during flight has been studied[15]. For the manipulation system as UAVs equipped with a gripper, contact forces and external disturbances acting on the gripper and the entire system should be considered[16, 1, 4]. And there have also been works using multiple collaborative UAVs in order to perform transportation tasks[7, 6]. However, when it comes to multiple UAVs carrying one payload, there are problems like the interactions between UAVs, physical couplings in the joint transportation of the payload and stabilizing the payload along three-dimensional trajectories. In these studies, single or a team of helicopters or quadrotors with grippers have been used to assist various manipulation tasks and yielded impressive results. But when trying to manipulate an object, these UAVs cannot exert arbitrary forces possibly applied to the object.

Because typical helicopters or quadrotors cannot instantaneously resist or apply an arbitrary force in the plane perpendicular to the rotor axis.

Typical quadrotors have four fixed pitch propellers with parallel (and vertical) thrust vectors. The four thrust actuators provide a mapping from 4-D actuator space to 6-D Cartesian force space with rank no greater than four. In fact, the standard quadrotor configuration results in rank of exactly four as the four thrusters provide linear force along Z, and torques around X, Y and Z. Torque around Z is achieved indirectly through coriolis forces resulting from differential angular velocities of the counter-rotating propellors. (This is what makes tri-rotors infeasible and conventional single-rotor helicopters also have four actuators: main rotor, tail rotor and two actuators on the swash plate.) Instantaneous exertion of linear forces along X and Y are impossible with these configurations (as are instantaneous velocities in X and Y, resulting in a nonholonomy).

Typical helicopters and quadrotors are inherently underactuated for their 6-DoF mobility of position and orientation in space. With only four independently controlled inputs, they cannot independently control UAV's position and orientation at the same time. To fix this problem, a quadrotor design with tilting propellers has been presented in [10]. With four additional actuators added for tilting propellers, the 'quad-tilt UAV' now has full control over its 6-DoF mobility. When the propellers tilt, all the thrusters become nonparallel. And developed about the same time as our design, a similar non-planar design called 'Tumbleweed' was introduced by the University of Manchester [5]. Using six variable-pitch/fixed-speed rotors, it is designed to truly achieve full flight envelope, as hover at any orientations and translate in any directions. In these two works, the actuation concept of tilting propellers during flight actually makes it possible to access all 6 degrees of freedom of the robot. But for aerial manipulation tasks, we want to exert forces as fast as possible to resist any arbitrary wrench. Tilting propellers during flight using servos may not be fast enough for our purposes. So each rotor on our hexrotor is pitched at an optimized angle based on specific task.

2 Design

To create six independent degrees of freedom in force/torque space, one must have at least six actuators. A conventional hexrotor has six parallel-thrust propellers spaced evenly around the circumference of a circle. Because all thrusters are vertical, no components of the six thrust vectors point along the X or Y axes; they all point out-of-plane, resulting in no in-plane components. So we rotate each thruster a cant angle ϕ around its radius to form a nonparallel design, in-plane components result while still maintaining a symmetric basis of vectors.

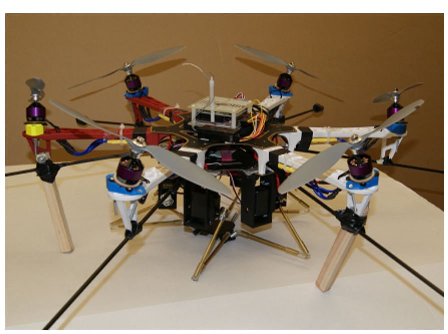

Figure 1: Flight-capable prototype of Dexterous Hexrotor with manipulator.

The motors are mounted on in house designed and fabricated ABS plastic adapters that canted at an optimized angle tangentially to the edge on the end of each arm. Position of six motors and their rotation are defined in Fig. 2. By alternating clockwise and counter-clockwise rotations, the torque each motor produced shares same direction with motor force's in-plane components, providing torque around Z axis. X configuration is chosen, so X axis aligns with $Motor_3$ and $Motor_6$.

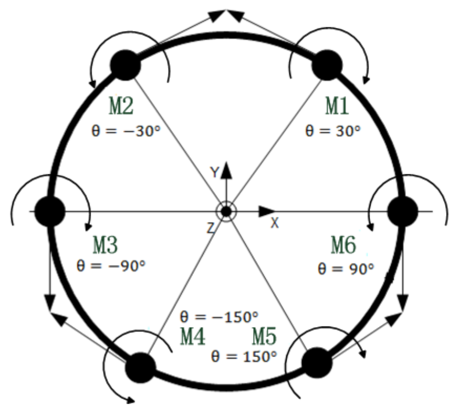

Figure 2: Motor definitions of Dexterous Hexrotor with rotation indicated, where n is the motor number, θ represents angular displacements of the motors.

2.1 Force Decomposition

The thrust and torque applied on the UAV by each motor can be expressed as

$$\begin{aligned} F_{motor} &= K_1 * PWM_{motor} \\ \tau_{motor} &= K_2 * PWM_{motor} \end{aligned} \tag{1}$$

where K_1 and K_2 are motor-dependent parameters and can be determined experimentally. PWM_{motor} is the command torque sent to the motor via Pulse Width Modulation (PWM).

To compute the net force/torque acting on the UAV from all thrusters, we first decompose each motor's thrust and torque into X, Y, and Z components on the body frame. The components of Cartesian generalized forces from $Motor_1$ can be put into a matrix as in equations (2) and (3).

$$\begin{bmatrix} F_{1fx} \\ F_{1fy} \\ F_{1fz} \\ F_{1\tau x} \\ F_{1\tau y} \\ F_{1\tau z} \end{bmatrix} = \begin{bmatrix} -K_1 * PWM_1 * cos(\theta_1) * sin(\phi) \\ K_1 * PWM_1 * sin(\theta_1) * sin(\phi) \\ K_1 * PWM_1 * cos(\phi) \\ d * K_1 * PWM_1 * cos(\theta_1) * cos(\phi) \\ -d * K_1 * PWM_1 * cos(\theta_1) * cos(\phi) \\ d * K_1 * PWM_1 * sin(\phi) \end{bmatrix} \tag{2}$$

$$\begin{bmatrix} \tau_{1\tau x} \\ \tau_{1\tau y} \\ \tau_{1\tau z} \end{bmatrix} = \begin{bmatrix} -K_2 * PWM_1 * cos(\theta_1) sin(\phi) \\ K_2 * PWM_1 * cos(\theta_1) sin(\phi) \\ K_2 * PWM_1 * cos(\phi) \end{bmatrix} \tag{3}$$

Where $[F_{1fx}F_{1fy}F_{1fz}F_{1\tau x}F_{1\tau y}F_{1\tau z}]^T$ are forces and torques decomposed from the thrust produced by $Motor_1$ and $[\tau_{1\tau x}\tau_{1\tau y}\tau_{1\tau z}]^T$ are Coriolis effects resulting from the torque produced by $Motor_1$. ϕ is the cant angle of each thruster and note that when ϕ is zero, the Coriolis effect only produces a yaw torque as with a normal quadrotor. θ represents the motor's position relative to the body and d is the radius of the UAV.

Then we compute the total force/torque $[F_{1x}F_{1y}F_{1z}\tau_{1x}\tau_{1y}\tau_{1z}]^T$ applied on the UAV by $Motor_1$ as

$$\begin{bmatrix} F_{1x} \\ F_{1y} \\ F_{1z} \\ \tau_{1x} \\ \tau_{1y} \\ \tau_{1z} \end{bmatrix} = \begin{bmatrix} F_{1fx} \\ F_{1fy} \\ F_{1fz} \\ F_{1\tau x} + \tau_{1\tau x} \\ F_{1\tau y} + \tau_{1\tau y} \\ F_{1\tau y} + \tau_{1\tau z} \end{bmatrix} = PWM_1 * \begin{bmatrix} -K_1 C\theta_1 S\phi \\ K_1 S\theta_1 S\phi \\ K_1 C\phi \\ C\theta_1(dK_1 C\phi - K_2 S\phi) \\ C\theta_1(-dK_1 C\phi + K_2 S\phi) \\ dK_1 S\phi + K_2 C\phi \end{bmatrix} \tag{4}$$

Once one motor is decomposed, we can follow the same pattern and decompose all six motors. Then we can combine these six 6x1 matrices into a 6x6 matrix which is the thrust to force/torque mapping, M_ϕ. With K_1 and K_2 determined for our motors, if the cant angle $\phi = 20°$, the thrust mapping is $M_{20°}$

$$M_{20°} = \begin{bmatrix} -1.69 & 1.69 & 0 & -1.69 & 1.69 & 0 \\ 0.97 & 0.97 & -1.95 & 0.97 & 0.97 & -1.95 \\ 5.36 & 5.36 & 5.36 & 5.36 & 5.36 & 5.36 \\ 1.21 & 1.21 & 0 & -1.21 & -1.21 & 0 \\ -0.7 & 0.7 & 1.4 & 0.7 & -0.7 & -1.4 \\ 0.65 & -0.65 & 0.65 & -0.65 & 0.65 & -0.65 \end{bmatrix} \tag{5}$$

which would conform to a nonparallel design. This matrix provides a mapping from 6-D actuator space to 6-D force/torque space and has a rank of 6, indicating we have 6 independent controlled degrees of freedom in Cartesian force/torque space.

To control the force/torque applied to the platform, the desired Cartesian force/torque vector is multiplied by the inverted thrust mapping matrix, producing a vector of PWM values (motor command torques) as in equation (6):

$$\begin{bmatrix} PWM_1 \\ PWM_2 \\ PWM_3 \\ PWM_4 \\ PWM_5 \\ PWM_6 \end{bmatrix} = [M]^{-1} \cdot \begin{bmatrix} F_x \\ F_y \\ F_z \\ \tau_x \\ \tau_y \\ \tau_z \end{bmatrix} \tag{6}$$

2.2 Control

A control system based on equation 6 for indoor human controlled flight has been developed as shown in Fig. 3. An attitude controller is used to stabilize the hexrotor for hunman controlled flight and control hexrotor's orientation. An position controller is implemented to control hexrotor's position. Hexrotor's attitude is measured by a 9 Dof IMU and its position in space is measured by an 8-camera Vicon MXT40 motion capture system.

Unlike common quadrotor, orientation and position control is separate in hexrotor's control system. τ_x, τ_y, τ_z are used to keep and adjust hexrotor's orientation. $[F_x F_y F_z]$ are used to

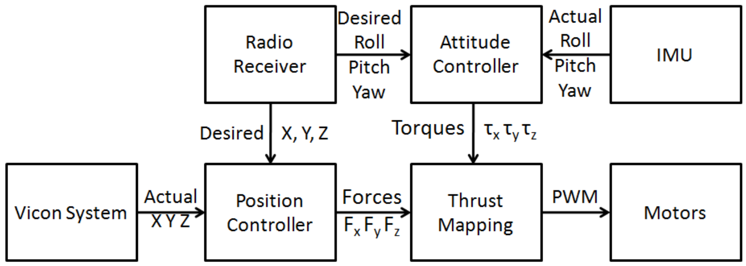

Figure 3: Hexrotor control system.

control hexrotor's thruster vector and maintain its position. SO when hexrotor's orientation is changed and tilting at an angle, its thruster vector will still point upward with adjustment of $[F_x F_y F_z]$ rather than point forward like a common quadrotor.

2.3 Optimizing the Cant Angle, ϕ

The cant angle ϕ decides how much force we can put into F_z, τ_x, τ_y or F_x, F_y, τ_z. Dependent on the motors we chosen, desired load of our manipulator and diameter of the UAV frame, we plot maximum forces and torques near hover condition at different cant angles in Fig. 4

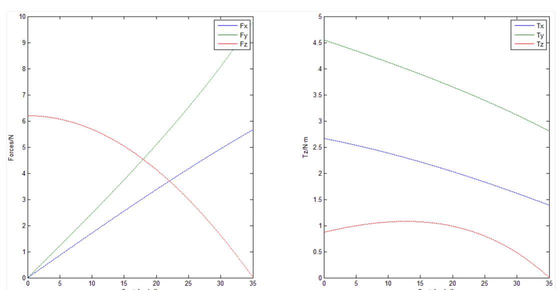

Figure 4: Maximum forces and torques near hover condition at different cant angles.

Clearly at $\phi = 0°$, there are no forces in X or Y and not much torques around Z. The opposite happens when ϕ is 35°, where all forces in Z are used to provide lift, but more force can be applied in X and Y.

To optimize the cant angle for the performance of our UAV, we adapt Yoshikawa's concept of "manipulability" to ours. As defined by Yoshikawa, "manipulability measure" is a quantitative measure of manipulating ability of robot arms in positioning and orienting the end-effectors, by looking at the isotropism of manipulator's motion in linear dimensions X, Y, Z and angles roll, pitch, yaw [17]. So for our UAV, we consider the combination of forces and torques as a similar measure of mobility. We are going to look at the isotropism of the forces and torques, not just how strong is it. To visualize how isotropic are the forces and torques, we plot these force/torque ellipsoids as shown in Fig.5.

When the cant angle is 0°, we get no ability to control F_x, F_y, but a lot of ability to control F_z. We also have ability to control τ_x, τ_y, τ_z, but not too much control over yaw because coriolis effect is weak. Then we cant the motor a little bit, we get a little bit control over F_x and F_y,

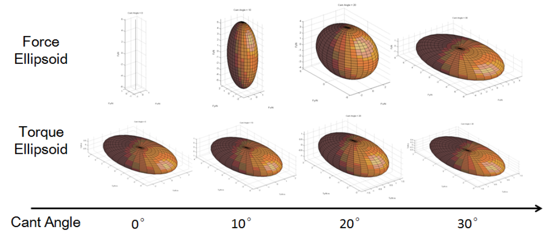

Figure 5: Force and Torque Ellipsoids at different cant angles.

but still very strong control in F_z. And likewise we get a little more control over τ_z. At 20°, the force ellipsoid becomes almost equal and the torque ellipsoid also gets more round. At 30°, the force ellipsoid gets flat and the torque ellipsoid starts to squash down again. Therefore we can see from 0° to 30° and beyond, the force/torque ellipsoid can get very isotropic at some point, which is good in our mobility measure.

We can also look at the condition number of the conversion matrix, which is the ratio of maximum eigenvalue to the minimum eigenvalue of the matrix. At 0°, when we have no control over F_x and F_y, the condition number becomes infinite, because two of the eigenvalues are 0. Then it can get smaller and smaller by increasing the cant angle, but eventually it will get higher again. Compared to a larger condition number, a small condition number means the same change in PWM would cause a smaller change in forces and torques, which is better to keep the UAV stable.

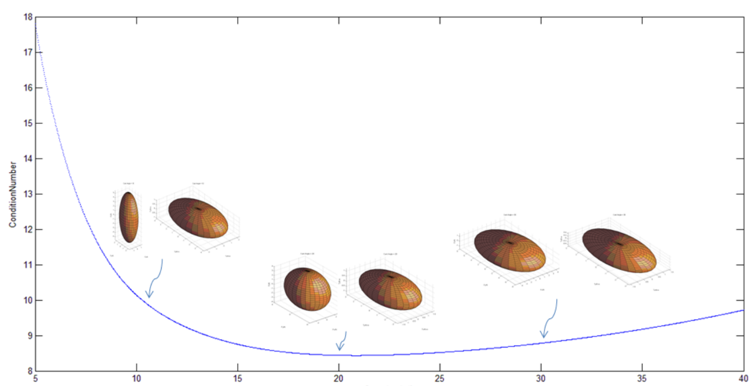

Figure 6: Condition number with force/torque ellipsoids.

We combine these two metrics on the same plot as shown in Fig. 6. We plot the condition number of the conversion matrix with force/torque ellipsoids at different cant angles, giving us a measure of the isotropism of our UAV. Therefore, dependent on the motors we have chosen, particular load of our manipulator, and diameter of the UAV frame, we optimize the cant angle at 20°. If we change the load, we would optimize this for a different cant angle.

2.4 Aerial Manipulator

To complete an aerial mobile manipulation system with the aerial mobile base described above, we have begun development of a lightweight, parallel HexManipulator. This 6-DoF end effector, which augments the 6-DoF of the hexrotor, will provide a macro/micro combination for enhanced performance. The HexManipulator will provide the fine adjustments at higher bandwidth that the coarse hexrotor is unable to do. We are developing the software infrastructure on our RecoNode CPU subsystem to control the UAV/manipulator combination in a macro/micro configuration using Khatibs Operational Space formulation [8]. This manipulator platform is similar to the configuration of Uchiyama's HEXA parallel robot[14], which provides a large workspace (for a parallel-chain manipulator) based on rotary actuators.

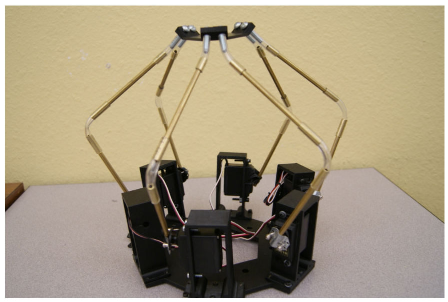

Figure 7: Hexrotor flying with manipulator.

There are six links, actuated by a rotary actuator, connecting the base and traveling plate. Each link is a serial combination of a 1 DoF active rotary joint, a 2 DoFs passive universal joint, and a 3 DoFs passive spherical joint. The link is composed of two rods connected by the universal joint and is connected to the base by the rotary joint while it is connected to the traveling plate by the spherical joint on the other end. The 2 DoFs universal joint is implemented with a length of flexible tubing and the 3 DoFs spherical joint is implemented with the same length of tubing plus a passive rotary joint that allows the tubing to twist freely.

3 Experiment

To test the response time of the Dexterous Hexrotor corresponding to external forces, a staged peg-in-hole task is presented with the hexrotor and a typical quadrotor from DIY Drones. A frame diagram as Fig. 8 shows the experiment's setup. Active control of the HexManipulator was not used in this test as the peg was held rigidly by the hexrotor. With the peg trapped half-way in a hole which is attached to a 6 DoFs force sensor, we start the UAV up and increase throttle until it can carry its own weight. Then we command both the hexrotor and quadrotor to exert a horizontal force perpendicular to the axis of the peg.

The result is shown in Fig. 9. Changes in force sensor measurements of Fy are direct measurements of the force which UAVs applied on the hole. A positive and a negative pulse are detected around 600ms and 1600ms. At the meantime, attitude of the UAVs was recorded and plot in the same figure.

The result shows that when both the hexrotor and quadrotor are able to exert same force in the plane perpendicular to the rotor axis, the hexrotor is much faster. This is because the hexrotor is exerting the force in a different way than common quadrotor. While quadrotor is

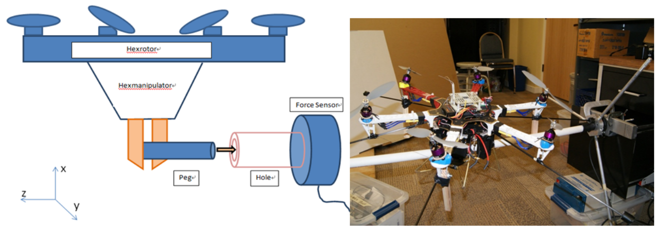

Figure 8: Peg-in-hole setup, with force sensor's coordinate system indicated.

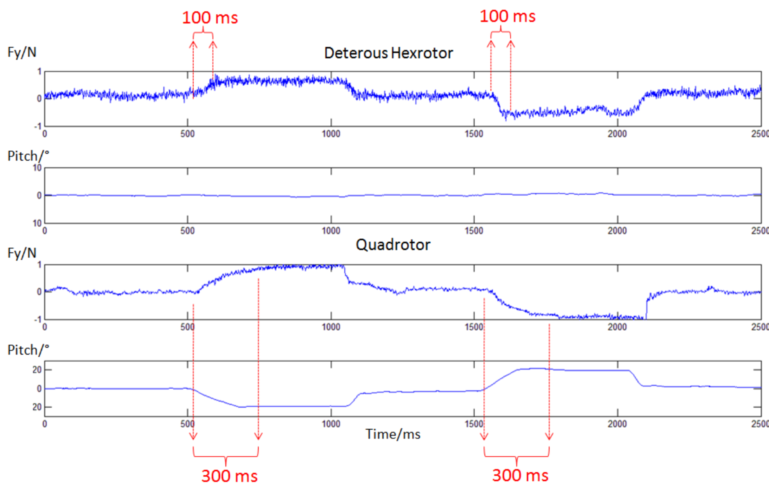

Figure 9: Hexrotor and quadrotor peg-in-hole measurements of F_y, Pitch.

tilting an angle to generate the horizontal force, the hexrotor can do it by simply changing the rotational velocity of the rotors without tilting. It is obvious that the lag varying speeds of propellers of the hexrotor will be much smaller that that caused by tilting the entire body of a quadrotor.

4 Conclusion

A truly holonomic aerial rotorcraft that provides force closure for controlled interaction with external structures has been introduced. The key contribution of this paper is to derive the thrust mapping based on decomposed net force/torque and develop a metric for the cant angle optimization of the dexterous UAV's performance for manipulation-based tasks. A flight-capable prototype has been built and tested.

It should be noted that we claim our hexrotor can "instantaneously resist arbitrary forces." This is not strictly true as the hexrotor can only change the torque of its motors instantaneously. The required change in the thrust magnitude is not dependent on torque, for a propeller, but on speed. Therefore, the independent thrust magnitudes and the resulting net force/torque experience a lag due to the inertia of the thrusters. The lag due to the rotor inertia is much smaller than that due to pitching the entire vehicle, as for a conventional quadrotor, and we believe is smaller than the pitching of the variable ϕ concept of the Tumbleweed (which also has to overcome the gyroscopic action of the rotors).

References

[1] S. Stramigioli A. Keemink, M. Fumagalli and R. Carloni. Mechanical design of a manipulation system for unmanned aerial vehicles. In *Proceedings, IEEE International Conference on Robotics and Automation*, 2012.

[2] A. Albers, S. Trautmann, T. Howard, T. Nguyen, M. Frietsch, and C. Sauter. Semi-autonomous flying robot for physical interaction with environment. In *Proceedings, IEEE International Conference on Robotics Automation and Mechatronics*, pages 441–446, June 2010.

[3] Antonio Bicchi. On the closure properties of robotic grasping. *International Journal of Robotics Research*, 14:319–334, August 1995.

[4] T. Danko C. Korpela and P. Oh. Mm-uav: Mobile manipulating unmanned aerial vehicle. In *Journal of Intelligent and Robotic Systems*, 2011.

[5] A. Scillitoe I. Lunnon A. Llopis-Pascual J. Zamecnik s. Proctor M. Rodriguez-Frias M. Turner A. Lanzon W. Crowther D. Langkamp, G. Roberts. Modeling and control of a quadrotor uav with tilting propellers. In *Proceedings, International Micro Air Vehicle conference*, 2011.

[6] N. Michael V. Kumar D. Mellinger, M. Shomin. Cooperative grasping and transport using multiple quadrotors. In *Distributed Autonomous Robotic Systems*, volume 83, pages 545–558, 2013.

[7] M. Bernard A. Ollero I. Maza, K. Kondak. Mechanical design of a manipulation system for unmanned aerial vehicles. In *Journal of Intelligent and Robotic Systems*, volume 57, pages 417–449, Jan 2010.

[8] O. Khatib. A unified framework of motion and force control of robot manipulators: The operational space formulation. In *IEEE Journal of Robotics and Automation*, volume RA-3, pages 43–53, 1987.

[9] C. Korpela and P.Y. Oh. Designing a mobile manipulator using an unmanned aerial vehicle. In *IEEE International Conference on Technologies for Practical Robot Applications*, April 2011.

[10] P. R. Giordano M. Ryll, H. H. Bulthoff. Modeling and control of a quadrotor uav with tilting propellers. In *Proceedings, IEEE International Conference on Robotics and Automation*, 2012.

[11] D. Mellinger, M. Shomin, N. Michael, and V. Kumar. Cooperative Grasping and Transport using Multiple Quadrotors. In *Proceedings of the International Symposium on Distributed Autonomous Robotic Systems*, Nov 2010.

[12] Nathan Michael, Soonkyum Kim, Jonathan Fink, and Vijay Kumar. Kinematics and statics of cooperative multi-robot aerial manipulation with cables. In *ASME International Design Engineering Technical Conference and Computers and Information in Engineering Conference*, 2009.

[13] V.-D. Nguyen. Constructing force-closure grasps. *International Journal of Robotics Research*, 7:3–16, June 1988.

[14] M. Uchiyama P. Maurine, D.M. Liu. Self calibration of a new hexa parallel robot. In *4th Japan-France Congress and 2nd Asia-Europe Congress on Mechatronics*, volume 1, pages 290–295, 1998.

[15] D. Bersak P. Pounds and A. Dollar. Grasping from the air: Hovering capture and load stability. In *Proceedings, IEEE International Conference on Robotics and Automation*, 2011.

[16] F. Ruggiero V. Lippiello. Mechanical design of a manipulation system for unmanned aerial vehicles. In *IEEE/RSJ International Conference on Intelligent Robots and Systems*, 2012.

[17] T. Yoshikawa. Manipulability of robotic mechanisms. In *Journal of Robotics Research*, volume 4, 1985.